# Role of the Steady-State $Na^+$ Channel Current in Pacemaker Depolarizations in Young Embryonic Chick Ventricular Myocytes

Hideaki Sada[1], Takashi Ban[1], Takeshi Fujita[2], Yoshio Ebina[2] and Nicholas Sperelakis[3]

[1]*Department of Pharmacology, School of Medicine and* [2]*Department of Electric Engineering, Fuculty of Engineering, Yamaguchi University, Ube 755, Japan*

[3]*Department of Molecular and Cellular Physiology, School of Medicine, University Cincinnati, Cincinnati, Ohio 45267, U.S.A.*

*Received June 8, 1995 Accepted July 31, 1995*

ABSTRACT—To assess the age-related changes in kinetic properties of the cardiac $Na^+$ channel, whole-cell voltage-clamp (v-c) experiments were conducted using 3-, 10- and 17-day-old embryonic chick ventricular heart cells. In line with the first-order kinetic model, kinetic parameters for the activation and inactivation of the channel were determined from the v-c results. Simulation studies using kinetic parameters so determined have reproduced the current-voltage relations and the steady-state inactivation characteristics observed in cells in the three age groups. The rate of depolarization of the simulated action potentials was also comparable to that experimentally recorded. In conclusion, the steady-state $Na^+$ conductance can play a significant role in the automatic depolarizations observed in young embryonic ventricular cells.

*Keywords*: Heart, Voltage-clamp, Development, Automaticity, Simulation

Depression of cardiac pacemaker activity is a common property shared among all class-1 antiarrhythmic agents (1), but it has been questioned if the major action of these drugs, their $Na^+$ channel blocking action, is responsible for the depression, since the $Na^+$ channels contribute little to the pacemaker depolarizations due to the low channel density as well as their inactivation in the range of pacemaker potentials.

The fast $Na^+$ channel properties change during development. Above all, the presence of the automatic activities and slow rate of rise of action potential (AP) in ventricular cells is characteristic only in an early stage of development (see ref. 2 for a review). In the previous voltage-clamp (v-c) study using cultured heart cells from 3-, 10- and 17-day-old embryonic chick ventricles (3), we quantified the developmental changes in the activation and inactivation kinetics parameters. In the study, we found that the steady-state (window) conductance of the $Na^+$ channel at ca. $-40$ mV in the young (3-day) heart was 0.6% of the maximum conductance ($g_{Na}$), and suggested that the current in this magnitude was large enough to induce the pacemaker depolarization. To provide evidence for the involvement of the window conductance in automatic depolarizations in this tissue, further v-c experiments were carried out for the three age groups, with special reference to the inactivation kinetics over a whole potential range, to enable the simulation study. We report here that the $Na^+$ window current plays an important role in the slow depolarization during the diastole in ventricular cells of young embryos.

## MATERIALS AND METHODS

### *Experimental procedures*

The hearts from 3-, 10- and 17-day-old chick embryos were dissected under sterile conditions. The procedures for cell separation and cultivation were similar to the previously reported ones (3–5). The use of fertilized eggs for the v-c experiments was approved and authorized by the Animal Experiment Committee, Yamaguchi University, School of Medicine. Glass pipette electrodes were fabricated by a two-step pulling of Pyrex glass capillary tubes (o.d. = 1.4 mm), and each electrode was coated with Sylgard up to near the tip. The tip of the pipette was carefully heat-polished. Single cells having a spherical shape (diameter of ca. 10–15 $\mu$m) were chosen for the study. Data sampling was carried out either at 50 kHz for v-c or 100 kHz for AP recordings. The signal of the time derivative (dV/dt) of AP was obtained by an opera nal amplifier, monitored on a cathode ray oscilloscope or fed into a computer via A/D conversion.

*Solutions and liquid junction potential*

The calcium ion was totally omitted from the bath solution. In the v-c experiments, but not in the AP recording experiments, K ion was replaced by equimolar Cs ion. The standard bath solution for v-c had the following composition: 140 mM NaCl, 5.4 mM CsCl, 1.1 mM $MgCl_2$, 10 mM HEPES and 10 mM glucose (pH=7.4). The bath temperature was controlled at 16–17℃ by a Peltier-effect unit. The composition of the internal (pipette) solution for v-c was: 130 mM Cs-aspartate, 11 mM EGTA, 1.0 mM $CaCl_2$, 10.0 mM HEPES, 2.0 mM $MgCl_2$, 5 mM ATP-$Na_2$ and 5 mM glucose (pH=7.2–7.3). The free $Ca^{2+}$ concentration in the pipette solution was estimated to be $3\times10^{-9}$ M. The liquid junction potential ($V_{lj}$) between the bath and pipette solutions was determined independently, assuming a negligible $V_{lj}$ for 3 M KCl (4). Voltage values reported herein were all corrected for the $V_{lj}$ of 15 mV.

*Passive electrical properties*

The membrane capacitance ($C_m$) was determined either from time integration ($\int I\cdot dt$) of the capacitive spike for 10-mV step pulses or from the current in response to ramp pulses (dV/dt=5 V/sec). The falling phase of the capacitative transients before compensation (upon 10-mV step pulses) was approximated by a single exponential function. The $R_s$ value was obtained from the time constant ($\tau$) of the exponential fit, which is given by $C_m\times R_s$. Based on such $C_m$ and $R_s$ values, the settling time (to 90% level) after each voltage step was calculated to be 90–260 μsec. Data were not used from experiments in which the voltage error due to $R_s$ exceeded 5 mV. $R_s$ was usually compensated to 60–70%. The residual (uncompensated) fraction of the capacitative transient was digitally corrected by means of the −P/4 method.

*Procedures for data analyses and simulations*

In the previous study (3), inactivation time constants at potentials positive to −40 mV were obtained simply by fitting the decaying time course of the current for the single exponential function. In the present study, the inactivation at potentials negative to −40 mV were assessed by a double-step pulse protocol (Fig. 1A, inset): the holding potential ($V_H$) was −120 mV, in which the inactivation must be totally eliminated. The extent of inactivation which develops during the 1st pulse ($V_1$) was examined by a successive 2nd pulse ($V_2$). Inactivation time courses were analyzed as a function of $V_1$ duration (t) by fitting to exponential functions. The envelope of the current peaks responding to $V_2$ steps was fitted by an exponential function. For such exponential fittings, non-linear least-square methods (simplex and Marquardt) were used.

Table 2 shows all equations (eqs. (1)–(6)) and parameter values required for simulation of both v-c data and AP data. The current-voltage (I-V) relation (Fig. 2) and the steady-state inactivation characteristics (Fig. 3) were reproduced by computation using eq. (1) in combination with:

$$m=m_\infty-(m_\infty-m_0)\times EXP(-t/\tau_m) \quad (7)$$

and

$$h=h_\infty-(h_\infty-h_0)\times EXP(-t/\tau_h) \quad (8)$$

Here, parameter values of m and h at t=0 ($m_0$, $h_0$) and t=∞ ($m_\infty$, $h_\infty$) and time constant values ($\tau_m$, $\tau_h$) at each voltage were given by eqs. (4) and (5), respectively. In v-c reproductions, the step in time was 0.05 msec.

The integration algorithm used to solve the differential equations for AP reproductions was the Runge-Kutta algorithm. In such AP simulations, the step in time was 0.01 msec.

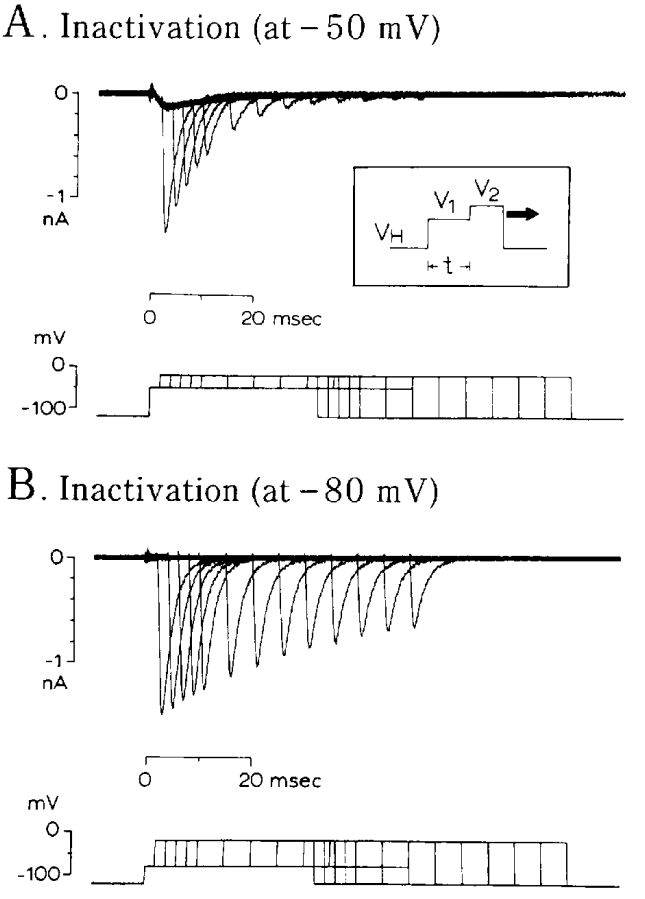


**Fig. 1.** Inactivation time courses and time constants of inactivation. Double-step pulse protocol (inset in panel A). The holding potential ($V_H$) was −120 mV, at which the inactivation is completely eliminated. The extent of inactivation that develops during test steps ($V_1$) was examined by applying 2nd pulses ($V_2$). The duration (t) of the $V_1$ pulse was stepwise lengthened in either a 2-msec (to 10 msec) or 5-msec (from 10 to 50 msec) increment. $V_1$=−50 mV (A) and −80 mV (B). The duration and voltage of $V_2$ was 30 msec and −20 mV, respectively. Pulse rate: 1/4 sec. 17-day-old cell, 17℃.

## RESULTS

### *Inactivation time constant*

The time courses of inactivation occurring at large membrane potentials (more negative than −40 mV) could be tested by a double-step pulse protocol (inset in Fig. 1A). Figure 1 shows instances of the time courses of inactivation developing during the $V_1$ pulse of −50 mV and −80 mV. The longer the $V_1$ duration (t), the smaller the current peaks responding to $V_2$ were. The time constants in any age group showed a bell-shaped voltage-dependence: peaked around −80 mV (3- and 10-day-old cell) or −90 mV (17-day-old cell) (data not shown). Table 1 shows the time constants of inactivation obtained through exponen-

**Table 1.** Time constant of inactivation (double-step protocol)

| $V_m$ (mV) | 3-Day | 10-Day | 17-Day |
|---|---|---|---|
| −100 | | 23.9±3.3 (3) | 38.1±1.1 (11) |
| −90 | 22.6±4.0 (3) | 36.7±1.5 (9) | 43.1±1.4 (13) |
| −80 | 38.5±1.6 (13) | 37.0±1.2 (12) | 35.0±1.7 (12) |
| −70 | 33.7±1.0 (14) | 29.1±0.6 (11) | 23.0±1.1 (9) |
| −60 | 22.2±1.1 (13) | 19.0±0.8 (9) | 14.4±0.9 (6) |
| −50 | 13.7±0.7 (9) | 10.8±1.0 (4) | 8.5 (2) |
| −40 | 8.6±0.7 (5) | | |

Values (in msec) are means±S.E.M. Number of observations is shown in parentheses.

**Table 2.** Equation and parameter values used for simulation study

A. Equation and values that define the $Na^+$ current

$$I_{Na}=\overline{g_{Na}}\cdot C_m\cdot m^3\cdot h\cdot(V_m-V_{rev}) \quad (1)$$

| | $g_{Na}$ (nS/pF) | $V_{rev}$ (mV) | $C_m$ (pF) |
|---|---|---|---|
| 3-Day | 0.74 | 65.0 | 8.0 |
| 10-Day | 2.65 | 65.0 | 8.0 |
| 17-Day | 5.40 | 65.0 | 8.0 |

B. Equations defining time derivatives

$$dV_m/dt=-(1/C_m)\times(I_{Na}-I_{external}) \quad (2)$$
$$dy/dt=(y_\infty-y)/\tau_y \quad (3)$$
$$y_\infty=\alpha_y/(\alpha_y+\beta_y) \quad (4)$$
$$\tau_y=1/(\alpha_y+\beta_y) \quad (5)$$

C. A defining function and values for rate constants (RC) ($\alpha$ or $\beta$)

$$RC=(C_1EXP(C_2(V_m+C_3))+C_4(V_m+C_5))/(EXP(C_6(V_m+C_3))+C_7) \quad (6)$$

| | RC ($msec^{-1}$) | $C_1$ ($msec^{-1}$) | $C_2$ ($mV^{-1}$) | $C_3$ (mV) | $C_4$ ($(mV\cdot msec)^{-1}$) | $C_5$ (mV) | $C_6$ ($mV^{-1}$) | $C_7$ |
|---|---|---|---|---|---|---|---|---|
| 3-Day | $\alpha_m$ | 0 | 0 | 38.7 | −0.12676 | 38.7 | −0.12676 | −1 |
| | $\beta_m$ | 0.04158 | −0.0556 | 0 | 0 | 0 | 0 | 0 |
| | $\alpha_h$ | $6.0\times10^{-1}$ | −0.063 | −79 | 0 | 0 | 0 | 0 |
| | $\beta_h$ | 1.1865 | 0 | 3.5 | 0 | 0 | −0.0593 | 1 |
| 10-Day | $\alpha_m$ | 0 | 0 | 34.2 | −0.17431 | 34.2 | −0.17431 | −1 |
| | $\beta_m$ | 0.05899 | −0.05337 | 0 | 0 | 0 | 0 | 0 |
| | $\alpha_h$ | $1.7\times10^{-6}$ | −0.054 | −82 | 0 | 0 | 0 | 0 |
| | $\beta_h$ | 2.33711 | 0 | −10 | 0 | 0 | −0.055 | 1 |
| 17-Day | $\alpha_m$ | 0 | 0 | 39.3 | −0.17431 | 39.3 | −0.17431 | −1 |
| | $\beta_m$ | 0.03894 | −0.0542 | 0 | 0 | 0 | 0 | 0 |
| | $\alpha_h$ | $3.6\times10^{-6}$ | −0.045 | −91 | 0 | 0 | 0 | 0 |
| | $\beta_h$ | 3.6 | 0 | −15 | 0 | 0 | −0.053 | 1 |

In eqs. (2)−(5), times (t, $\tau$) are in msec, membrane capacity is in pF, rate constants ($\alpha$, $\beta$) are in $msec^{-1}$. Equations (3)−(5) show the method of computing the dimensionless conductance parameters using y to represent such parameters (m, h). $I_{external}$ is the current to displace the membrane potential toward the positive potential direction (cf. legends for Fig. 4).

tial fittings. Calculations by the least-square method using such time constants at large potentials (Table 1) and time constants of the current-decay upon single-pulse steps (Fig. 5 in Ref. 3), in combination with the steady-state inactivation ($h_\infty$) data (3), yielded the rate constant (RC) of inactivation. Table 2C shows the RC values as related to voltage according to eq. (6) ($\alpha_h$ and $\beta_h$). Such voltage-related RCs were used for later simulation studies.

*Simulation*

Reproductions of results on v-c and APs were carried out using the parameter values listed in Table 2, and Table 2 also shows the equations involved (eqs. (1)–(6)). The first step in the simulation was to determine RC values such as $\alpha_m$, $\beta_m$, $\alpha_h$ and $\beta_h$ corresponding to each potential. Parameters, $C_1$–$C_7$ for RCs of $\alpha_m$ and $\beta_m$ (Table 2C) and values for the maximal conductance ($\overline{g_{Na}}$), reversal potential ($V_{rev}$) and membrane capacitance ($C_m$) (Table 2A) rely on the results reported previously (3).

*Current-voltage (I-V) relation:* Figure 2 shows the computed I-V relations for 3-, 10- and 17-day-old embryonic cells. The currents were computed in response to voltage steps of increasing amplitude in either 5 mV (from −50 to 0 mV)- or 10 mV (from 0 to 70 mV)-increments from a holding potential ($V_H$) of −90 mV. In the I-V data of the previous study (3), the currents reached the peak values of 228 pA (n=11) at the voltage step to −17 mV, 675 pA (n=14) to −18 mV and 867 pA (n=12) to −16 mV, for 3-, 10- and 17-day-old cells, respectively. These are in accordance with the reproduction results here. Hence, the parameter values we obtained are adequate.

*Steady-state inactivation ($h_\infty$):* Based on the values in Table 2 (A and C), the steady-state inactivation was computed for the three groups (Fig. 3). Current peaks plotted

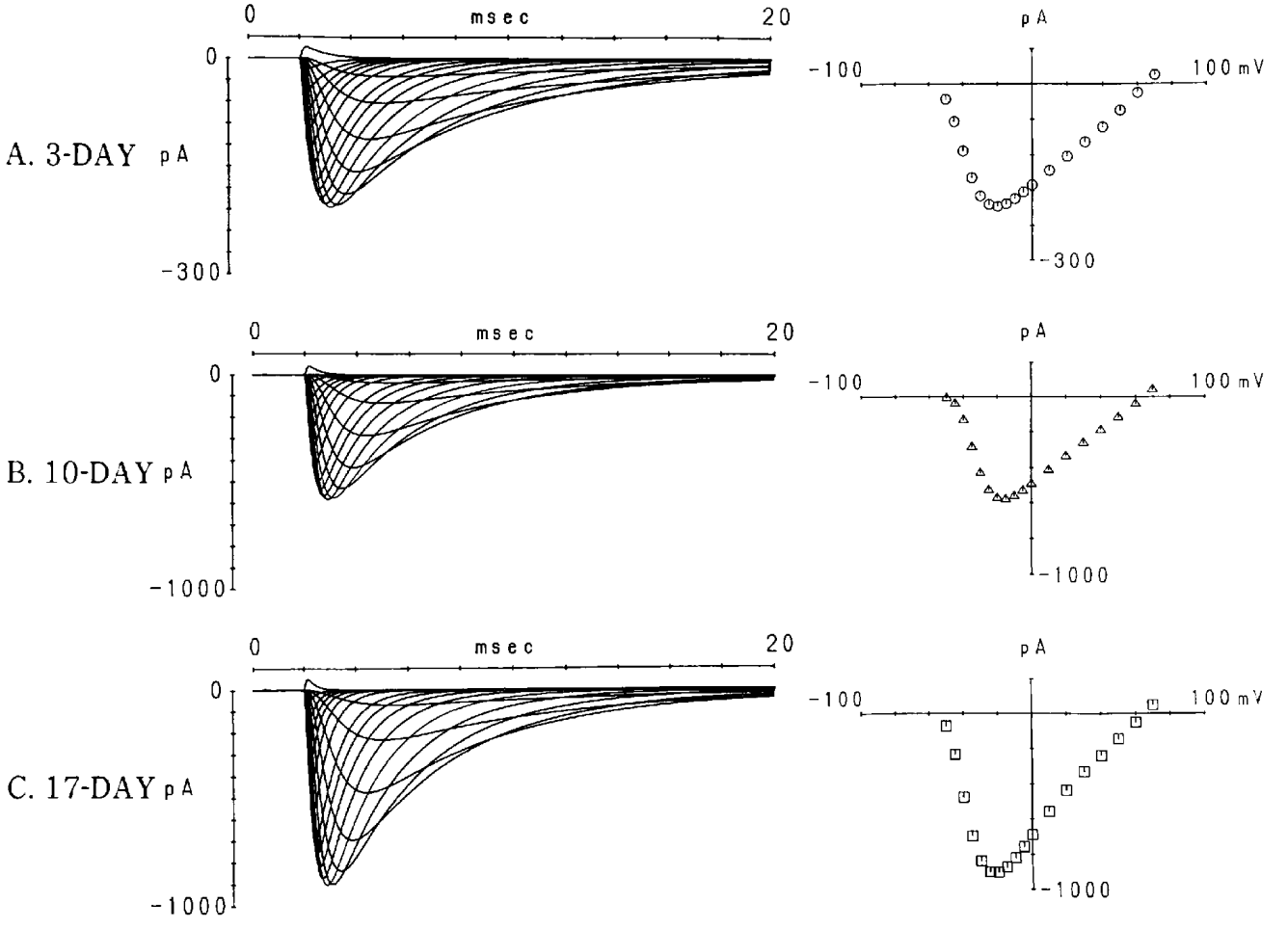


**Fig. 2.** Computed current-voltage (I–V) relation. A: 3-day-old cell, B: 10-day-old cell, C: 17-day-old cell. Left: Superimposed traces of currents responding to voltage steps of varying amplitude, Right: I–V plot. Note the difference in current scale. $V_H = -90$ mV. All parameters required for the computations are presented in Table 2 (A and C). Equations involved in the simulations are shown in Table 2 (A, B and C).

against the conditioning voltage demonstrated a sigmoidal relation to voltage (right). Approximations of these current peaks by the Boltzmann equation (eq. (9)) gave the half inactivation voltages ($V_{1/2}$) and slope factors (S):

$$h_\infty = I_{Na(max)}/(1+EXP(V_m - V_{1/2})/S)) \quad (9)$$

While the slope factors (ca. 10 mV) were unchanged, the half inactivation voltage changed in development from −79.4 mV (3-day) through −83.9 mV (10-day) to −91.0 mV (17-day). These values also are comparable to those in the previous study (3): −78 mV, −83 mV and −91 mV, for 3-, 10- and 17-day-old cells, respectively.

*Action potential:* The transmembrane potential was recorded at 17℃ for the three groups in the presence of the normal $K^+$ concentrations in the bath (5.4 mM) and pipette (ca. 140 mM) solutions.

In half of the 3-day-old cells, spontaneous but sporadic APs were observed every 4−10 sec for the first 1−5 min after ruptures of the patched membrane. The spontaneous activity tended to depress with time, so that the membrane potential ($V_m$) often showed damped oscillations and resided around −20 mV thereafter. In the other half of the cells, APs were never emitted and $V_m$ also resided around −20 mV. In the spontaneously firing ventricular cells, the maximum diastolic potentials (MDP), when monitored on a cathode ray oscilloscope, were between −40 and −50 mV. The maximum rate of rise of APs ($\dot{V}_{max}$) was 1−2 V/sec.

In contrast, ventricular cells from 10- and 17-day-old embryos were electrically silent but capable of generating APs upon current-pulse stimuli, the resting membrane potentials (RMP) of which were −60 to −65 mV and ca.

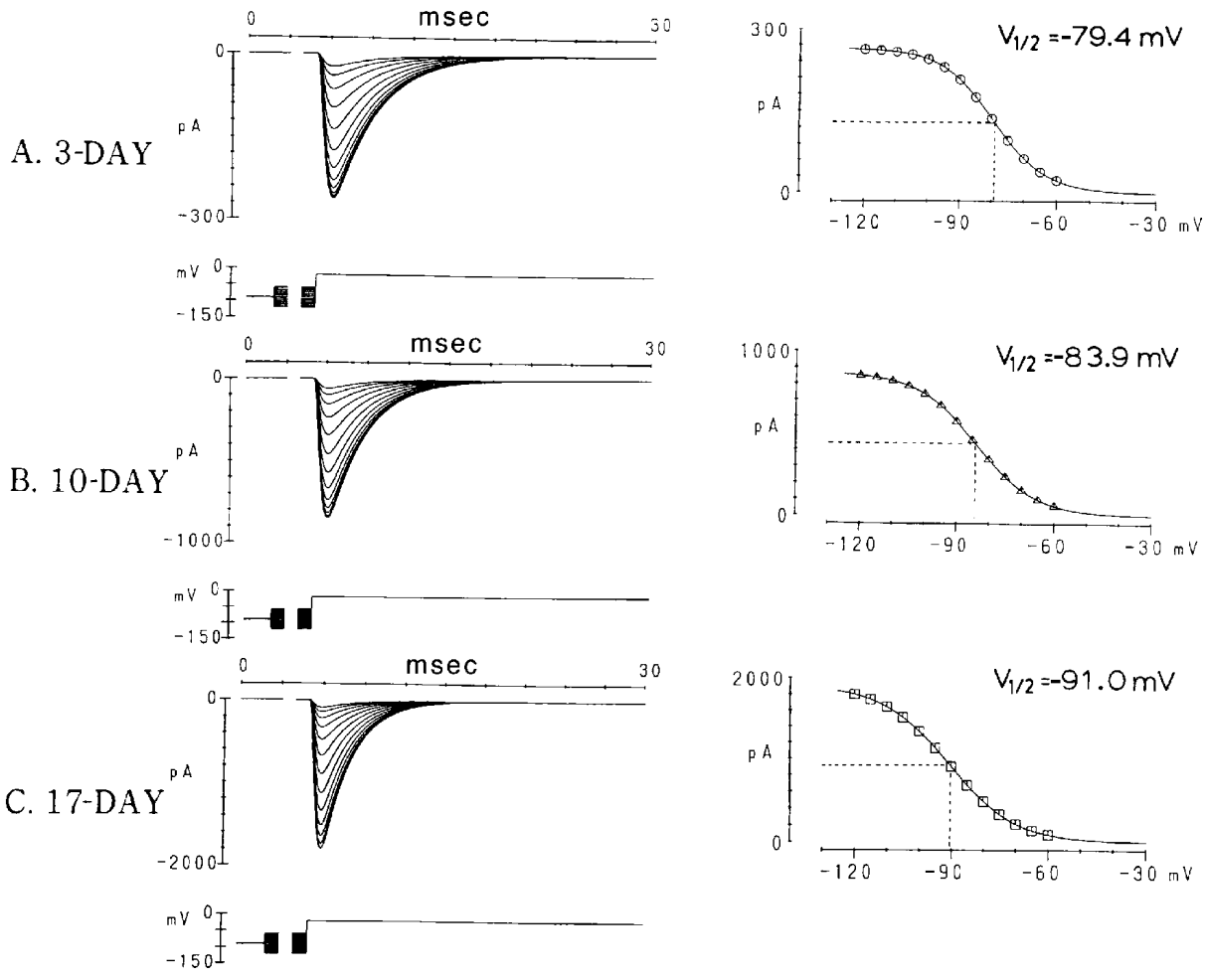


**Fig. 3.** Computed steady-state inactivation. A: 3-day-old cell, B: 10-day-old cell, C: 17-day-old cell. Left: Superimposed $Na^+$ currents responded to 2nd pulses. The duration of the prepulse is infinite and its voltage was increased stepwise from −120 to −60 mV in 5-mV steps. Right: Plot of current peaks (in pA) against prepulse voltage ($h_\infty$ relation). The smooth curves were drawn according to the Boltzmann equation (eq. (9)) by non-linear least-squares fitting. Broken lines denote the half inactivation voltage ($V_{1/2}$) of the relation.

$-70$ mV in 10- and 17-day-old cells, resectively. The $\dot{V}_{max}$ was 10–20 V/sec in 10-day-old and 20–30 V/sec in 17-day-old cells.

Using the values shown in Table 2 (A–C), the time courses of change in $V_m$ were computed for the three age groups (Fig. 4). In the computations, currents from other types of channels were not taken into account. In simulations for cells of day 3, $V_m$ was set at $-50$ mV (close to the MDP), at the start. In the absence of any current from other origins, the membrane progressively depolarized by the residual (steady-state) $Na^+$ current alone. Here, the maximum rate of depolarization ($\dot{V}_{max}$) of 0.34 V/sec was seen at $-40$ mV, at which $h=0.014$, $m=0.675$, and the resultant $Na^+$ conductance in the $m^3$ model, in turn, corresponds to only to 0.4% of $\overline{g_{Na}}$. However, the residual $Na^+$ current of this magnitude was sufficient for a slow

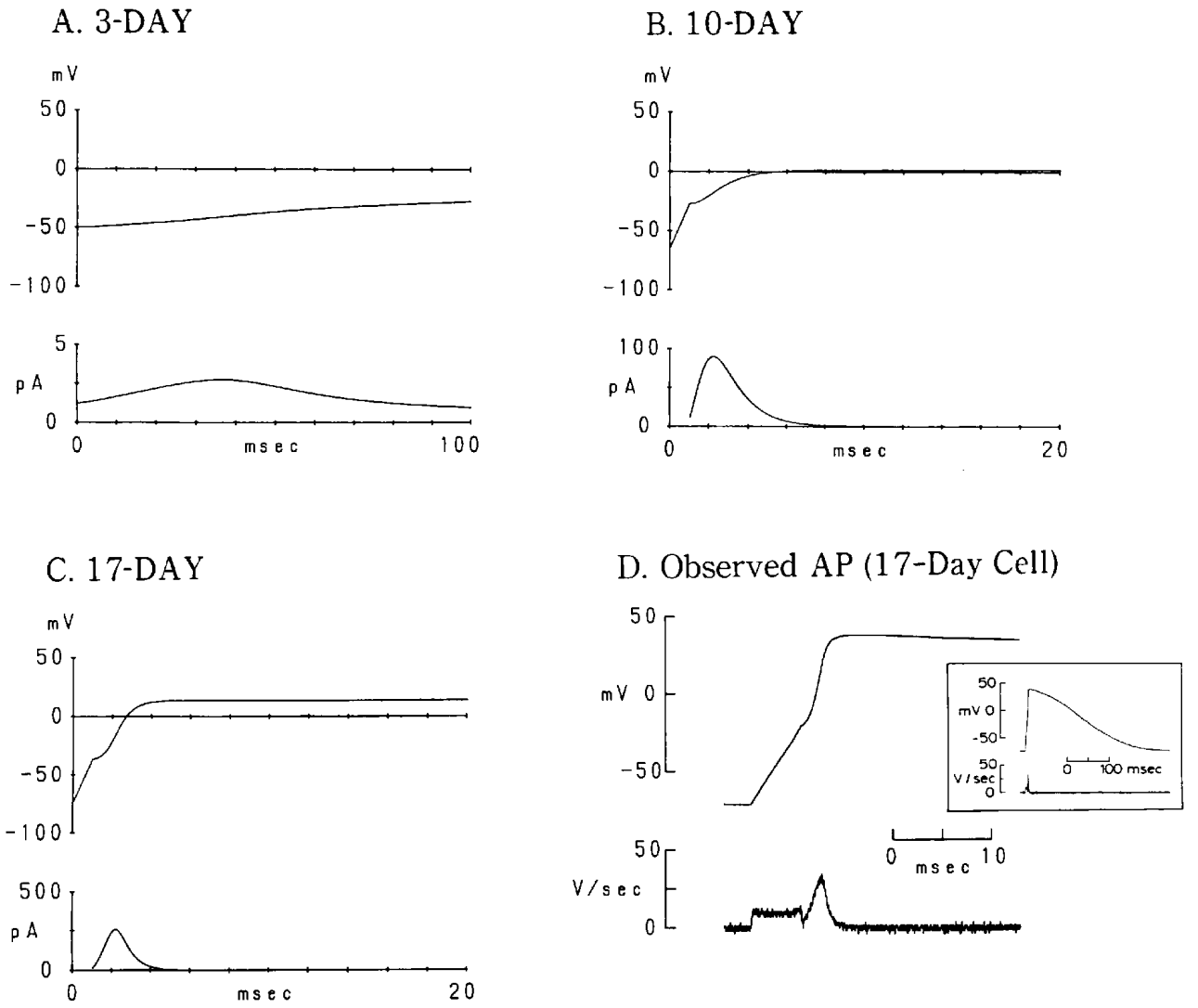


**Fig. 4.** Simulated time course of depolarization induced by the $Na^+$ current and an experimentally-recorded action potential (AP). Simulations in A–C were carried out by the Runge-Kutta method, using eqs. (1)–(8). Table 2 (A and C) shows the parameter values required for the computations. Currents from other types of channels are not taken into account. A: 3-day-old cell. Depicted is a time course of the spontaneous voltage change computed when the start voltage was set at $-50$ mV without externally applied current. The maximal current (2.7 pA) appearing at $-41$ mV induces the maximum rate of rise of depolarization ($\dot{V}_{max}$) of 0.34 V/sec. B: 10-day-old cell. The trace is the time course of $V_m$-change when the start voltage is $-65$ mV and the external current ($I_{external}$, 0.3 nA, 1 msec) is given. C: 17-day-old cell. A computation of the time course of the potential change after an external current ($I_{external}$, 0.3 nA, 1 msec) is applied. The starting voltage is set at $-74$ mV, the same as in D). D: An experimentally recorded AP from a 17-day-old embryonic ventricular cell ($C_m=8.7$ pF). The upstroke phase of the AP is shown in an expanded time scale. The upper trace is AP and the lower trace is its time derivative (dV/dt). Inset: Whole time courses of AP (upper trace) and dV/dt (lower trace). RMP $=-74$ mV, Maximal dV/dt $=34$ V/sec.

membrane depolarization. As a result, $V_m$ reached −28 mV within 100 msec after the start of simulation even at a low temperature of 17℃ (Fig. 4A).

Predicted time courses of $V_m$ change were also computed for 10- (Fig. 4B) and 17-day-old cells (Fig. 4C). In contrast to the 3-day-old cell result, $V_m$s for the latter 2 groups remained unchanged for at least 10 sec, as long as $V_m$s were initially set near their RMP: −60 mV (10-day) and −70 mV (17-day). However, the external application of current was followed by rapid rises of the potential (Fig. 4, B and C). In these cells, the $V_{max}$ of 11.2 V/sec and 32.5 V/sec (Fig. 4C) were attained at −17.8 mV and −15.0 mV, for 10- and 17-day-old cells, respectively. For comparison, Fig. 4D shows a representative AP observed experimentally in 17-day-old cells. At 17℃, the RMP and the $\dot{V}_{max}$ of this cell were −74 mV (the same as in simulated APs (Fig. 4 C)) and 34.0 V/sec, respectively.

The $\dot{V}_{max}$ of the simulated AP is comparable to that of the observed APs, although in the simulations, the currents derived from other channel types were not involved. Taking all the above findings into consideration, it can be concluded that in young embryonic ventricular cells, the membrane can rapidly depolarize by virtue of the residual $Na^+$ conductance alone from the MDP to a certain potential level close to the threshold voltage for the 2nd inward ($Ca^{2+}$) current (discussed later).

## DISCUSSION

Ventricular cells in 3-day-old embryos exhibit automatic depolarizations, the rate of which is 3−15 mV/sec (6). The automaticity in these cells progressively subsides over the whole process of development towards electrical silence as seen in adult cells (2). The ionic background of such an automaticity in young cells has not been well-understood (7). In the previous study (3), we found that the steady-state (window) $Na^+$ conductance in ventricular cells of the young (3-day-old) embryonic cells is fairly large, compared to those of the aged (10- and 17-day-old) cells, suggesting a relevance of the window conductance to the automaticities. To obtain all kinetic parameters required for simulating AP, further whole-cell v-c experiments were made for the three age groups.

In the present study, the time course of AP was not completely reproduced because little quantitative information was available about currents from other sources such as $Ca^{2+}$ and $K^+$ channels. Nonetheless, using these experimentally-determined kinetic parameters, not only v-c results for the three groups, but also early (rising) phases of APs for 10- and 17-day-old cells could be reproduced well.

In young embryonic ventricles, slow diastolic depolarizations of around −40 mV were generated, possibly even by the steady-state $Na^+$ current alone. However, this does not seem to be the case for the 10- and 17-day-old cells, since the window conductance per se is relatively low, and since the membrane potentials also are large. Although the membrane potential ($V_m$) under simulations with the Runge-Kutta method must reach the reversal potentials ($V_{rev}$, +65 mV) sooner or later, $V_m$ in any age group actually failed to reach them soon, tended to stop depolarizing at a certain voltage level (Fig. 4, A−C) and hover thereafter around −20 to −30 mV for day 3, and 0−10 mV for days 10 and 17. These $V_m$ values are much lower than those of the crest potential (i.e., +30 to +40 mV) of experimentally observed APs at 17℃ but rather near the activation voltage for the $Ca^{2+}$ channels (8). This implies that 1) the crest of APs in such cells are induced by inward currents from ion channels of different types (likely $Ca^{2+}$ channels) rather than $Na^+$ channels, and 2) importance of the $Na^+$ current in the cells is in moving $V_m$ for the successive activation of $Ca^{2+}$ channels.

The maximum rate of rise ($\dot{V}_{max}$) of simulated APs for the 10- (11.2 V/sec, Fig. 4B) or 17-day-old (32.5 V/sec, Fig. 4C) cell was comparable to the $\dot{V}_{max}$ of recorded APs, whereas $\dot{V}_{max}$ in simulated AP for the 3-day-old cell (0.34 V/sec) is much smaller than that observed experimentally (ca. 1−2 V/sec at 17℃). Hence, the rapid upstroke phase of APs is attributed to the fast $Na^+$ current in the older cells but is attributed to the Ca inward current in the young cells. This deduction is in accordance with the findings that in 3-day-old ventricular tissues, the $Na^+$ channel blocker tetrodotoxin (TTX) little (2) or slightly (9) altered the $\dot{V}_{max}$ of APs, but this toxin apparently slowed down the pacemaker activity (10).

The simulation procedures in the present study were based on $m^3$, instead of $m^1$ kinetics. Mitsuiye and Noma (11, 12) recently proposed the $m^1$ model for voltage-clamped mammalian (guinea pig) ventricular cells in the oil-gap method. In the previous study (3), we reported 3.57 as the m-exponent value for the embryonic chick ventricular cell. We recently confirmed in a theoretical study that the determination of the exponent value by the least-square method is affected by two factors, the cell membrane capacitance ($C_m$) and the series resistance ($R_s$) of v-c circuits (prepared for publication). At present, it remains to be decided whether a kinetic model of the $Na^+$ channel should adopt $m^1$ kinetics, as far as cardiac tissues are concerned.

A conclusion that the TTX-sensitive $Na^+$ channel current possibly influences the automaticity in ventricular cells is unique. Of course, this does not necessarily exclude the possibility that other currents such as $i_f$ current also may contribute to the pacemaker depolarizations in the ventricular cells of young embryos. However, the $i_f$ current in this tissue likely flows in a more negative

potential range ($V_m < -60$ mV) (7, 13).

The steady-state activation ($m_\infty$) curve starts rising at ca. $-70$ mV and increases thereafter in a sigmoidal fashion as the $V_m$ becomes positive. In contrast, the steady-state inactivation ($h_\infty$) curve starts rising at $-50$ to $-60$ mV and increases as the $V_m$ becomes negative. As a result, there is the overlap (window conductance) between the two curves that peaks around $-40$ mV. The window conductance-related depolarizations do not likely take place in the normal adult heart tissues as long as the RMP maintains a large value by virtue of the $K^+$ conductance. However, whenever RMP in an area in the heart is depolarized to ca. $-40$ mV, the window conductance no longer can be ignored. In this sense, antiarrhythmic drugs of an $Na^+$ channel-blocker-type might suppress the automaticity through this mechanism. In fact, such drugs are known to shift the h curve towards a negative potential direction. Such shifts in the h relation, in turn, result in a reduction in the magnitude of the window current.

REFERENCES


1 Campbell T: Differing electrophysilogical effects of class 1A, 1B and 1C antiarrhythmic drugs on guinea pig sinoatrial node. Br J Pharmacol **91**, 395–401 (1987)

2 Sperelakis N: Physiology and pharmacology of developing heart cells. Pharmacol Ther **22**, 1–39 (1983)

3 Sada H, Ban T, Fujita T, Ebina Y and Sperelakis N: Developmental change in fast Na channel properties in embryonic chick ventricular heart cells. Can J Physiol Pharmacol (in press)

4 Sada H, Kojima M and Sperelakis N: Use of single heart cells for the $Na^+$ current measurements. Mol Cell Biochem **80**, 9–19 (1988)

5 Sada H, Kojima M and Sperelakis N: Fast inward current properties of voltage-clamped ventricular cells of embryonic chick heart. Am J Physiol **255**, H540–H553 (1988)

6 Sperelakis N and Lehmkuhl D: Effect of current on trans-membrane potentials in cultured chick heart cells. J Gen Physiol **47**, 895–927 (1964)

7 Brochu RM, Clay JR and Shrier A: Pacemaker current in single cells and in aggregates of cells dissociated from the embryonic chick heart. J Physiol (Lond) **454**, 503–515 (1992)

8 Tohse N, Meszaros J and Sperelakis N: Developmental changes in long opening behavior of L-type $Ca^{2+}$ channels in embryonic chick heart cells. Circ Res **71**, 376–384 (1992)

9 Ishima Y: The effect of tetrodotoxin and sodium substitution on the action potential in the course of developnment of the embryonic chiken heart. Proc Jpn Acad **44**, 170–175 (1968)

10 McDonald TF, Sachs HG and DeHaan RT: Development of sensitivity of tetrodotoxin in beating chick embryo hearts, single cells and aggregates. Science **176**, 1248–1250 (1972)

11 Mitsuiye T and Noma A: Exponential activation of the cardiac $Na^+$ current in single guinea pig ventricular cells. J Physiol (Lond) **453**, 261–277 (1992)

12 Mitsuiye T and Noma A: Quantification of exponential $Na^+$ current activation in *N*-bromoacetamide-treated cardiac myocytes of guinea pig. J Physiol (Lond) **465**, 245–263 (1993)

13 Satoh H and Sperelakis N: Identification of the hyperpolarization-activated inward current in young embronic chick heart myocytes. J Dev Physiol **15**, 247–252 (1991)